Research Article

For reprint orders, please contact: reprints@futuremedicine.com

Nanomedicine

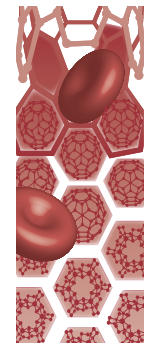

PEGylated crosslinked hyaluronic acid nanoparticles designed through a microfluidic platform for nanomedicine

Aim: A high versatile microfluidic platform is proposed to design, in a one-step strategy, PEGylated crosslinked hyaluronic acid nanoparticles (cHANPs) entrapping a magnetic resonance imaging contrast agent and a dye for multimodal imaging applications. **Materials & methods:** Clinically relevant biomaterials were shaped in the form of spherical NPs through a microfluidic flow focusing approach. A comparison between post processing and simultaneous PEGylation is reported to evaluate the potentiality of the chemical decoration of the cHANPs in microfluidics. **Results:** An accurate control of the NPs in terms of size, PEGylation and loading was obtained. Furthermore, *in vitro* cell viability is reported and their ability to boost the magnetic resonance imaging signal is also confirmed. **Conclusion:** The proposed microfluidic approach reveals its ability to overcome several limitations of the traditional processes and to become an easy-to-use platform for theranostic applications.

First draft submitted: 30 March 2017; Accepted for publication: 14 June 2017; Published online: 17 August 2017

Keywords: magnetic resonance imaging • microfluidics • nanoparticles

Maria Russo[1,2], Anna Maria Grimaldi[3], Paolo Bevilacqua[3], Olimpia Tammaro[1,2], Paolo Antonio Netti[1,2] & Enza Torino*[,1,2]

[1]Center for Advanced Biomaterials for Health Care, Istituto Italiano di Tecnologia, IIT@CRIB, Largo Barsanti e Matteucci, 80125 Naples, Italy

[2]Department of Chemical Engineering, Materials & Industrial Production, University of Naples Federico II, P.le Tecchio 80, 80125 Naples, Italy

[3]IRCCS Fondazione SDN, Istituto di Ricerca Diagnostica e Nucleare, 80143 Naples, Italy

*Author for correspondence: Tel.: +39 08119933100 enza.torino@iit.it

Traditional approaches for generating nanoparticles (NPs) by the solvent displacement route, are conventionally performed by bulk polymer nanoprecipitation process, in other words, by mixing the two phases in a batch vessel. Even though these technologies present numerous advantages such as the possibility to treat high volumes, they also suffer from serious drawbacks, such as poor flexibility of the formulation process and control of the NPs size, low tunability of the process in real-time [1,2]. In the nanomedicine field, special attention should be paid to the precise control of the physicochemical properties of the formulated NPs to achieve an optimal biodistribution. Furthermore, significant aspects comprise surface functionalization, like coating with polyethylene glycol (PEG) or targeting agents, high payload capability and controlled drug release. For all these aspects, the nanoprecipitation process must be reproducible and robust. Under these requirements, new possibilities to control NP formation by the nanoprecipitation route have emerged from microfluidic solutions [3,4].

Microfluidic approaches permit synthesizing micro and nanostructures having a narrow size distribution and further enable to easily guarantee high encapsulation efficiency and stable crosslinking reaction [5–7]. Among the several benefits that microdimension of microfluidic devices provides [8,9], there is also the ability to use products libraries of different materials rapidly by changing composition and flow rates. Indeed, the production of particles having a coefficient of variation (defined as the ratio between size' standard deviation and mean *100) is less than 5% and high encapsulation efficiency is efficiently achieved; furthermore, parallelization on microfluidic chips allows high throughput and multiple analysis and reaction at a time [10].

Future Medicine part of fsg

In this perspective, Karnik *et al.* [11] synthesized biodegradable PLGA–PEG polymeric NPs through a hydrodynamic flow focusing by nanoprecipitation where particle size and drug loading can be varied by flow rates, polymer composition and concentration. Later [12,13], a similar flow focusing microfluidic device, controlling the nanoprecipitation, showed that the co-encapsulation of hydrophilic and hydrophobic anticancer drugs with high encapsulation efficiency, platinum prodrug and docetaxel, respectively. Very recent studies on such technology reported potential *in vivo* applications with hybrid/PLGA NPs designed as therapeutic and imaging agents [14]. In another detailed microfluidic study, Capretto *et al.* [15] presented the formation of block copolymer stabilized NPs (hybrid NPs), by examining the effects of operational fluidic conditions and the feed concentration of polymers and actives on the size characteristics and the polymer coverage of the organic actives. Pluronic F127 was used as a model block copolymer while highly hydrophobic β-carotene was used as a model drug. Results demonstrated the existence of competitive reactions leading to the formation of two types of NPs, in other words, either with or without loading β-carotene in the core–shell structure. Other microfluidic-based nanoprecipitation processes are reported using another biocompatible and biodegradable polymer that is chitosan, but this time playing on the aqueous solubility of the polymer as a function of the pH. Chitosan presents a pKa around 6.2 at room temperature and thus, once solubilized at low pH, the mixing with a basic solution through microfluidic channels may induce the polymer nanoprecipitation. This idea was reported in recent articles [16,17], using hydrophobically modified chitosan, that is, by grafting palmitic acid on primary amines of chitosan with activation of acid by N-hydroxysuccinimide esters. The produced NPs were ranging in size between 50 and 300 nm and served to precisely encapsulate and release active hydrophobic principle (paclitaxel) over 1 week.

Nanoprecipitation processes in such devices open new benefits and new advantages regarding size control, drug encapsulation control and improvement [18–20].

In our recent work [21], we explored novel microfluidic strategies rationally designed to synthesize crosslinked hyaluronic acid nanoparticles (cHANPs) down to 50 nm to be applied in magnetic resonance imaging (MRI). A tight control of the nanoprecipitation behavior, of the crosslinking reaction and of the encapsulation efficiency of the MRI contrast agents (CAs), Gd-DTPA is reached.

MRI was selected because it is a routinely applied diagnostic modality, due to its noninvasivity and ability to obtain 3D tomographical information of soft tissues. Furthermore, it can be used for visualizing functions of cardiac, brain and central nervous system, as well as detecting tumor [22]. However, this technique suffers from the lack of sensitivity and information obtained from a simple unenhanced magnetic resonance image and, consequently, more than 35% of all clinical MRI scans utilize CAs to improve these aspects by selectively relaxing the water molecules near the complex [23].

Gadolinium-based CAs are the most used in the clinical MRI with over 10 million contrast enhanced MRI scans every year, because of their relatively high stability and inertness in the body even if they still lack in tissue specificity and exhibit low relaxivity [23]. Moreover, they could cause adverse effects, such as nephrotoxicity [24] and also the risk of intracranial deposition has been recently reported [25] earning the attention of the US FDA.

In these perspectives, several strategies have been investigated to overcome limitations of the clinical relevant CAs using nanotechnology [26–33]. However, the use of the microfluidic approaches to design nanostructures able to tune the relaxometric properties of the clinically approved CAs for MRI was still missing [21].

Herein, starting from the evidence of the previous work [21,34], the same microfluidic platform is enforced to entrap several diagnostic agents within the cHANPs simultaneously for multimodal imaging applications. Furthermore, a new combination of biomaterials, thiolated hyaluronic acid (HA-SH) and mPEG-vinylsulfone (PEG-VS), is also presented by optimizing the same microfluidic approach, proving the versatility of the proposed microfluidic platform by applying our strategies to different materials. In this last case, the simultaneous reaction of the HA-SH and PEG-VS to produce in a one-step strategy the PEGylated cHANPs encapsulating directly one or more active compounds is therefore carried on and size, shape and *in vitro* relaxivity analysis are also reported. Finally, a comparison between the traditional PEGylation of the cHANPs and the PEGylated cHANPs produced by the one-step strategy is reported.

Materials & methods

Materials

Sodium hyaluronate (M_w = 42 kDa) was purchased from Bohus Biotech (Strömstad, Sweden). Hyaluronate thiol (HA-SH), (M_w = 50 kDa) and mPEG-vinylsulfone (PEG-VS), (M_w: 2kDa), was purchased from Creative PEGWorks. Diethylenetriaminepentaacetic acid gadolinium(III) dihydrogen salt hydrate Gd-DTPA (M_w = 547.57 g/mol); Acetone (CHROMASOLV, for HPLC, ≥99.8%; molecular formula

CH_3COCH_3; M_w = 58.08); ethanol (ACS reagent, ≥99.5% (200 proof), absolute; molecular formula CH_3CH_2OH; M_w = 46.07); divinyl sulfone (or vinyl sulfone) (DVS) contains <650 p.p.m. hydroquinone as inhibitor; purity 97%; density 1.117 g/ml at 25°C (lit.); molecular formula $C_4H_6O_2S$; M_w = 118.15 mp); Sodium hydroxide NaOH (ACS reagent, ≥97.0%, M_w = 40.00); ATTO633 652 g/mol were purchased by Sigma-Aldrich Co (MO, USA). PEG–fluorescein isothiocyanate (FITC) (M_w = 1 kDa) is purchased from Nanocs Inc. (NY, USA); HRP-conjugated streptavidin, 1-Ethyl-3-(3 dimethylaminopropyl)-carbodiimide and N-hydroxysuccinimide and streptavidin (1 mg/ml) were purchased from Sigma-Aldrich Co. Cy7-PEG1KDa-NH_2 and Fitc- PEG1KDa-NH_2 were purchased from Nanocs Inc. The WST-1 assay was purchased from Sigma-Aldrich Co. The water, used for synthesis and characterization was purified by distillation, deionization and reserve osmosis (Milli-Q Plus; Merck, Darmstadt, Germany).

Microfluidic set-up for flow focusing approach

A quartz microfluidic device 'Droplet - Junction Chip' (depth × width 190 µm × 390 µm), purchased from Dolomite Centre Ltd, was used. The device has a flow focusing geometry with a 90° angle between the inlets to enhance the diffusion process [21]. On the chip, there are two separate droplet junctions, which can be used in combination. For all experiments, we have used only X-junction with three inlet channels and a single outlet channel that can be used to mix and react three reagents. A schematic representation was presented in Figure 1.

Preparation of cHANPs

Different flow rates were tested and the influence of the flow rate ratio, defined as the ratio of volume flow rate solvent and volume flow rate nonsolvent, was determined. For the feasibility study, an aqueous solution containing HA concentrations ranging from 0.01 to 0.1% wt/v was tested. The initial solution was kept under continuous stirring for at least 4 h and then injected through the middle channel. The flow rate of the middle channel was kept constant unvaried at 30 µl/min. Acetone, used as nonsolvent and injected through the side channels, was laterally injected to induce nanoprecipitation by a flow focusing approach. A total of 4% v/v DVS, used as a crosslinker for HA, was mixed with acetone before injecting within the microfluidic device. The flow rates of the side channels were constantly at 110 µl/min. Precipitated NPs were collected in a Petri glass containing about 25 ml of nonsolvent and kept under continuous stirring. Each experiment was repeated at least ten-times.

Simultaneous encapsulation of Gd-DTPA & fluorophores

Several concentrations of fluorophores at least 1 nmol/100 µl, ATTO633 and ATTO488, were mixed with HA aqueous solution together with Gd-DTPA at 0.1% wt/v.

Loading capability and encapsulation efficiency were calculated by Induced Coupled Plasma (ICP-MS) - NexION 350. NPs were suspended in a solution of deionized water at a concentration of 150,000 particles/ml. All data were collected and processed using the Syngistix Nano Application Module. Gd was measured at m/z 157 using a 100 µs dwell time with no settling time.

Stability & swelling behavior of cHANPs

ICP-MS was used to assess one-half of the solution for the total concentration of Gd^{3+} ions loaded within the NPs. The other half of the solution was filtered using 0.45 µm filter and the filtrate was analyzed for Gd^{3+} ions. The concentration of loaded fluorophore was determined using spectrofluorimeter ($\lambda_{ex/em}$ 488–550 nm).

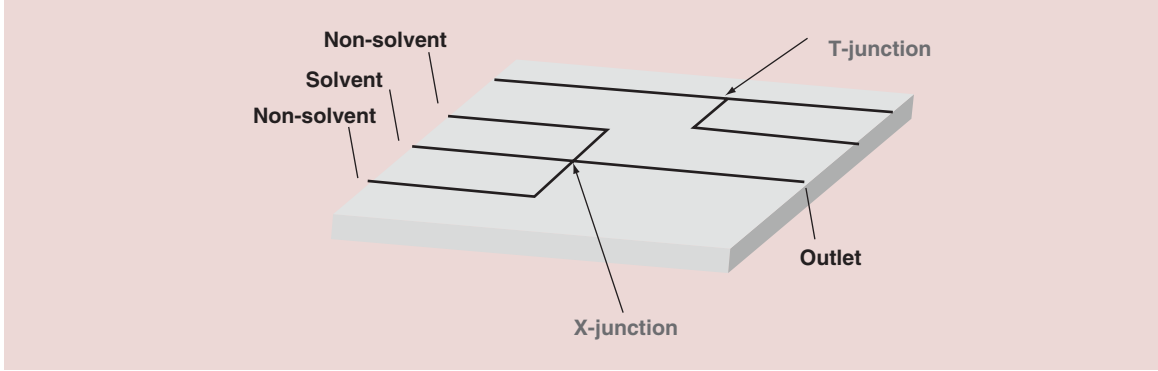

Figure 1. Microfluidic device. A schematic representation of the 'Droplet Junction Chip: 190 µm' with two configurations T- and X- junction, which can be used in combination.

In vitro cytotoxicity of cHANPs

An adenocarcinomic human alveolar basal epithelial cells (A549) was used. The cells were cultured in Dulbecco's modified Eagle's medium containing 10% fetal bovine serum and L-glutamine (2.9 mg/ml) at 37°C in water-saturated air supplemented with 5% CO_2. For the cytotoxicity measurements, the cells were plated in 96-well plates for 24 h before the addition of the NPs. Fresh medium containing an increasing concentration of NPs was added to each well and the cells were incubated for 24 h. At the end of the incubation time, the cytotoxicity of the NPs was tested using an WST-1 assay (Sigma-Aldrich, MI, USA). Briefly, phosphate-buffered saline (PBS) containing WST-1 was added to each well and the cells were incubated for 30 min, 1, 2, 4, 12 and 24 h. Spectral absorption of the samples was measured at 450 nm with ELISA Reader (Biotek, VT, USA). The number of live cells is proportional to the amount of formazan produced.

Quantification of carboxyl groups on the surface of cHANPs

Back titration method was performed to directly quantify carboxylic groups on the surface of cHANPs. In brief, 10 ml of cHANPs (0.1 mg/ml) was dispersed in 20 ml of 0.01 M NaOH solution, stirred for 30 min and then pH annotated. A standard solution of 0.01 mM HCl, was used as the titrant. After each addition of titrant the solution was stirred magnetically for 1 min and the pH was recorded. From the difference of NaOH and HCl concentration at equivalent point, the molar concentration of carboxylic sites was calculated. The titration was repeated on a second NP sample to check for reproducibility.

Conjugation with PEG-NH_2-Dye

The formation of an amide bond between the COOH groups on the NP surface and the NH_2 end groups of the PEG labeled with fluorophore was adopted as a strategy of attack to carry out the reaction of direct PEGylation. Especially for each reaction, PEG1KDa amino and labeled with different fluorophores (Cy7-PEG1KDa-NH_2 and FITC-PEG1KDa-NH_2) were used. The activation of the carboxylated surface of the cHANPs occurred after contact for 10 min with 500 µl of the starting sample to a solution of 1-Ethyl-3-(3 dimethylaminopropyl)-carbodiimide (230 µl at 70 mM) and N-hydroxysuccinimide (230 µl at 21 mM). Thereafter, 2mM of NH_2-PEG1KDa-Dye was added, allowing to react in the dark for 4 h and in a slight rotation. The excess reagents were removed by ultracentrifugation (30,000 r.p.m., 15°C, 10 min) or spin-x corning system (4000 r.p.m., 20°C, 10 min) and the pellet was suspended in a phosphate buffer (pH 6.8). The amount of reagents was stabilized basing on the quantification, carried out by titration of the carboxyl groups available on the surface of the cHANPs.

Quantification of PEG concentration

The amount of PEG conjugated to cHANPs was determined by spectrofluorimetric (ENSPIRE Multimode Plate Reader PerkinElmer). All measurements were performed in triplicate. The calibration line was set in the range of 0–80 nmol/ml (Ex/Em 480–550).

Synthesis of PEGylated crosslinked nanoparticles by nanoprecipitation in microfluidics in a one-step manner

For the feasibility study, an aqueous solution containing thiolated HA (HA-SH) concentrations ranging from 0.01 to 0.1% wt/v was tested. The initial solution was kept under continuous stirring for at least 4 h and then mixed with PEG-vinylsulfone (PEG-VS) (ranging from 0.4 to 1% v/v) at neutral pH and at 4°C to avoid the crosslinking reaction before nanoprecipitation occurs within the microfluidic device. Then, HA-SH and PEG-VS solution was injected through the middle channel. The flow rate of the middle channel was kept constant at 30 µl/min. Acetone, used as non-solvent and injected through the side channels, was laterally injected to induce nanoprecipitation by a flow focusing approach. The flow rates of the side channels were unchanged at 110 µl/min. Precipitated NPs were collected in a Petri glass containing about 25 ml of nonsolvent and kept under continuous stirring. In the literature studies, hydrogels between HA-SH and PEG-VS were obtained through a Michael addition in PBS at 37°C. The molar ratio of thiol groups to vinylsulfone groups was kept at 1.2 [35,36]. In our microfluidic platform, a study on the reagents was conducted to create, at the nozzle section, the nucleophilic addition of a carbanion (HA-SH) to unsaturated carbonyl compound (PEG-VS). Several experiments were carried out to promote the reaction and to reduce suddenly growth's step after the nucleation phase. Each successful experiment was repeated at least ten-times.

Purification and characterization of nanoparticles

A Spectra Por Cellulose Membrane 6 (Molecular Weight Cut Off MWCO 50,000) was used for purification protocol. A typical procedure consists of loading collected samples into dialysis tube and keeping the buffer solution under continuous stirring at 130 r.p.m. The concentration gradient of water was slowly added to the buffer solution to avoid aggregation and diffusion phenomena across the membrane. Dynamic light scattering was used to determine NP size. NPs were con-

centrated by ultracentrifugation or by rotavapor R-300. The recovery was performed at 15°C, at 60000 r.p.m. for 10 min. After these treatments, a 100 µl of purified samples were deposited on a polycarbonate Isopore Membrane Filter (0.05 and 0.1 µm) by ultrafiltration vacuum system. The precipitated or deposited particles were gold palladium coated, and a ULTRA PLUS field emission scanning electron microscope (FE-SEM Carl Zeiss, Oberkochen, Germany) was used to observe particles' morphology. Transmission electron microscope (TEM), stimulated emission depletion (STED) were also used to characterize the samples.

In vitro MRI of Gd- loaded PEGylated cHANPs

Empty NPs and Gd-DTPA loaded NPs were tested by *in vitro* MRI and results were compared with Magnevist and Gd-DTPA in water as a control. After vigorous stirring, changes in relaxation time (T_1) were evaluated at 1.5 Tesla by Minispec Bench Top Relaxometer (Bruker Corporation) by adding 300 µl of the sample in a glass tube [37]. The relaxation time distribution was obtained by CONTIN Algorithm. The relaxation spectrum was normalized on the CONTIN processing parameters. The integral of a peak corresponds therefore to the contribution of the species exhibiting this peculiar relaxation to the relaxation time spectrum [38]. Experiments were repeated at least five times.

Fourier transform infrared spectroscopy

Fourier transform infrared spectra (FT-IR) were collected from Nicolett 6700 FT-IR spectrometer (Thermo Scientific). All the IR spectra of the specimen were collected at 0.09 cm^{-1} resolution with 2 min interval. Thiolated HA, mPEG-Vinylsulfone and PEGylated cHANPs were analyzed to confirm if the reaction has taken place. Spectra were recorded and analyzed for signal assignation.

Results

Simultaneous encapsulation of different agents within the cHANPs

A schematic representation of the microfluidic device is reported in Figure 1. The same X-junction chip is used to perform all the experiments.

To produce cHANPS for multimodal imaging applications, an HA solution containing a model dye (ATTO633 or ATTO488), at 1 nmol/100 ml, and Gd-DTPA at 0.1% wt/v is added to the middle channel. No influence on the nanoprecipitation and crosslinking reaction is observed and, consequently, the flow focusing behavior is kept at *standard condition* (HA 0.05% wt/v and solvent flow rate 30 µl/min – nonsolvent flow rate 110 µl/min), as defined in our previous work [21].

FE-SEM characterization confirms the NP' size of about 40 nm even after several days in water (Figure 2A) while STED image of cHANPs (Figure 2B) loaded with ATTO633 and Gd-DTPA shows the encapsulation of the fluorophore.

Batch PEGylation reaction of cHANPs

To reduce potentially adhesive interactions of colloids with intracellular components *in vivo*, the surface of cHANPs has been coated with PEG. In the design of NPs for both drug-delivery and imaging applications, the addition of PEG to NPs represents a crucial step to reduce reticuloendothelial system uptake and increases circulation time versus uncoated counterparts. Indeed, the PEGylation has several advantages: a prolonged residence in the body, a decreased degradation by metabolic enzymes and a reduction or elimination of protein immunogenicity.

Using back titration, the concentration of carboxylic groups is determined by making them to react with an excess volume of base solution at a known concentration and then titrating the resulting mixture with the standardized acid solution. To optimize PEGylation reaction, we first perform quantitative characterization of carboxyl functionalities of cHANPs. Using back titration, we can quantify the number of surface functionalities, providing important information about the surface physicochemical properties and the effects on the quality and reproducibility of the functional nanomaterial. We estimate about 15 nmol of carboxylic group/mg of NPs.

As expected, PEGylation produces a chemical decoration of the particles inducing a larger NP size distributions due to the PEG-corona. Indeed, the measured size of the cHANPs decorated with PEG-FITC (1 KDa) is of about 60 nm diameter. However, it represents a significant result to prove the stability of the cHANPs undergone to chemical decoration and the possibility to maintain the dimension of the cHANPs under 100 nm preserving potentially a uniform *in vivo* biodistribution. Previously ζ-potential results demonstrated that cHANPs have a negatively charged surfaces (-40 mV), attributed to the presence of deprotonated carboxyl groups of HA. In details, PEGylation reduces the carboxylic groups from 15 ± 2.5 to 7 ± 1.5 nmol/ml, proving that some COOH– groups have not reacted or not directly exposed on the NP surface for PEGylation. However, as expected, the ζ-potential of the NPs was slightly decreased by PEGylation (-15 mV), due to the reduction of the carboxylic acids of HA. PEGylation is also useful to assess the surface stability of the NPs during the chemical decoration and the ability to retain the loaded Gd compound during the bioconjugation. This result places cHANPs as a good candidate for the delivery of active compounds on a specific target.

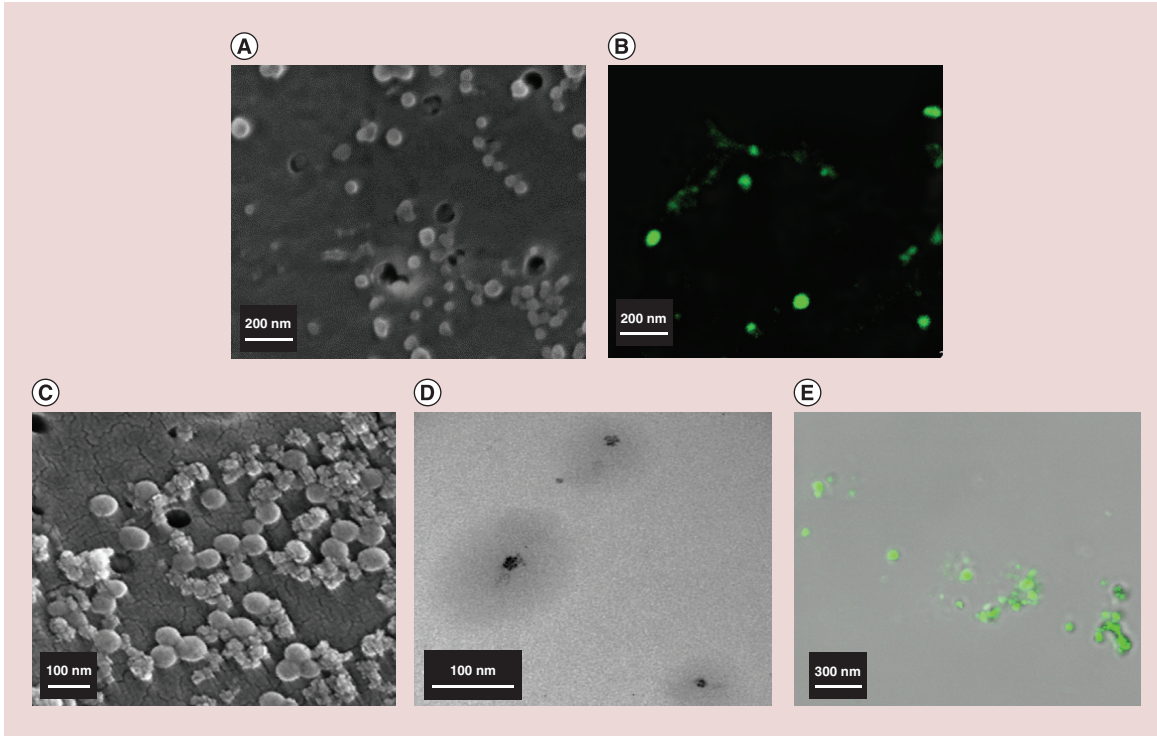

Figure 2. Simultaneous encapsulation of different agents within the crosslinked hyaluronic acid nanoparticles.
(A) FE-SEM and **(B)** STED images of cHANPs loaded contemporary with ATTO633 and Gd-DTPA after 48 h in water. Batch PEGylation reaction. **(C)** FE-SEM **(D)** TEM **(E)** STED images of loaded cHANPs after conjugation reaction with PEG_{1000}-FITC at *standard process conditions* after 48 h in water.
cHANP: Crosslinked hyaluronic acid nanoparticle; FE-SEM: Field emission scanning electron microscope; STED: Stimulated emission depletion; TEM: Transmission electron microscope.

SEM, TEM and STED images of cHANPs after PEGylation reaction are reported in Figure 2C, D & E. cHANPs subjected to direct PEGylation have maintained their spherical structure despite the presence of a higher surface roughness and a slight increment in size due to the chemical decorations.

In vitro cytotoxicity of nanoparticles

Typically, structural alterations of NPs in aqueous solutions, in cell-culture medium, might also affect and change the final results of the *in vitro* toxicological studies. Therefore, cytotoxicity tests are essential to assess preliminarily the biocompatibility of the cHANPs after the process. Understanding the behavior of NPs at the time of toxicological assay may play a crucial role in the interpretation of its results. The mechanical stability and the enzymatic degradation of the NPs are determined by the degree of crosslinking of HA structures. As highlighted by studies of Lai, HA sheets incorporated different concentrations of DVS in a range between 0 and 50 mM had a good cytocompatibility[2]. For this study, the toxicity of loaded cHANPs is tested using a WST-1 assay, which is based on the conversion of a water-soluble tetrazolium salt (yellowish in color) to water insoluble formazan (purple color) by living cells. Scalar concentrations of cHANPs are tested in a range between 10 and 100 μg/ml. It is evident that the cHANPs showed no detectable cytotoxicity *in vitro* (Figure 3).

The varied NP–cellular localization and interaction might lead to various modes of toxicity. Even NPs of the same material can show completely different intracellular behavior due to, for example, slight differences in surface coating, charge and size. It has been reported that especially the NP size determines the efficiency of cellular uptake and subsequent intracellular processing.

The disruption of the NPs inside the cell greatly influences the resulting toxic effects. The cytotoxicity could be attributed to the chemical composition of the nanostructure, but it should be considered that the NPs destabilization results in the release of their content into intracellular compartments, which can present synergic cytotoxic effects. This cytotoxicity can be desired, in antitumor treatments, or undesired during NPs application for diagnostics purposes. Furthermore, an excellent cell uptake of the NPs guarantees the efficient cell MRI and intracellular drug delivery. Preliminary cytotoxicity results on cHANPs are promising to improve the application of the nanomedicine in the diagnostic field.

Synthesis of PEGylated crosslinked nanoparticles by nanoprecipitation in microfluidics in a one-step manner

While in the above reported paragraph the PEGylation has been performed and optimized after the synthesis and the purification of Gd-loaded NPs. In this session, we intend to demonstrate the versatility of our designed microfluidic platform by synthesizing PEGylated cHANPs (PEG-cHANPs) in microfluidics through a co-nanoprecipitation process of HA-SH and PEG-VS at the same condition just used to produce cHANPs but avoiding the batch pegylation reaction of our NPs.

In this perspective, we have also obtained HA-PEG hydrogels NPs (of about 70 nm) using as aqueous solution 0.05% wt/v thiolated HA (HA-SH) and 0.8% v/v PEG-vinylsulfone (PEG-VS). This further study enables the exploitation of PEG coating and the effects of the nanoprecipitation on the flow-focusing behavior exclusively due to the presence of another polymer with non-negligible molecular weight (PEG-VS = 2 KDa). As expected, lower concentrations of PEG-VS lead to the formation of swelling particles while higher concentrations provoke uncontrolled precipitation of PEG-VS and flow instability.

In our microfluidic device, at the nozzle section, an effective nucleophilic addition of a carbanion (HA-SH) to unsaturated carbonyl compound (PEG-VS) should be achieved (Figure 4A).

TEM and FE-SEM images of the collected morphologies are showed in Figure 4B & C, respectively. We can observe that collected NPs maintain their shape even after 48 h in water due to a strong crosslinking reaction performed together with nanoprecipitation, encapsulation of Gd-DTPA and PEGylation of cHANPs. TEM image Figure 4B shows a different electron density between the core and the shell, that can give a previous indication of the presence of an outer covering coating different from the cHANPs before the PEGylation.

Fourier transform infrared spectra

FT-IR analysis is performed to confirm the effectiveness of the reaction. Comparative FTIR spectra of HA-SH, PEG-VS and PEGylated cHANPs are showed in Figure 5. The analysis shows that the PEGylated cHANPs do not exhibit the double bond C = C, observed for PEG-VS at 750 cm^{-1}, due to the Michael addition reaction between the double bond of the PEG-VS and thiol group of HA. Furthermore, the success of the reaction is also guaranteed by the presence of the peak at 600 cm^{-1} that indicates the C-S bond stretching. Nevertheless, results on PEGylated cHANPs also present the peak at 1245 cm^{-1} associated with C-SH vibration [39] related to the residual *not reacted* thiols of the precursor HA-SH. Further details are reported in Supporting Information.

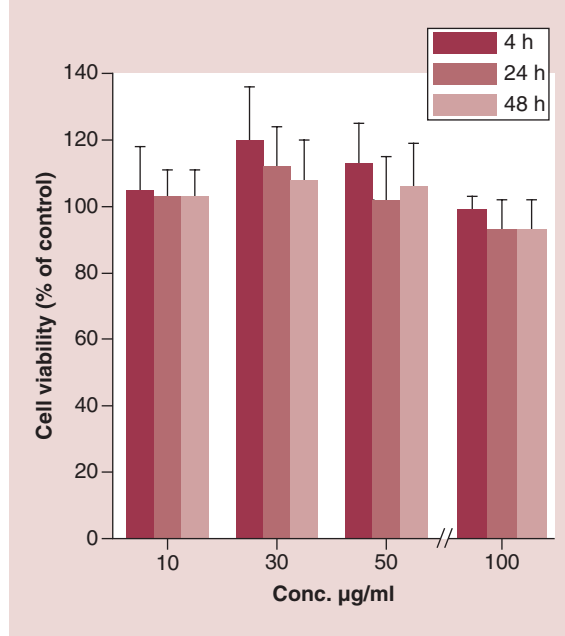

Figure 3. *In vitro* cytotoxicity. A549 cell viability expressed as a percentage of the value obtained with a concentration of cHANPs in a range between 10 and 100 µg/ml for three different time intervals. The error bars represent the standard deviations calculated from three independent experiments.
cHANP: Crosslinked hyaluronic acid nanoparticle.

FT-IR analysis finally reports that microfluidic platform to produce PEGylated cHANPs can accurately control the tuning of the crosslinking reaction to improve relaxometric properties and stability of the system.

In vitro MRI of Gd-loaded PEGylated cHANPs

In vitro relaxivity is studied for loaded and unloaded cHANPs and the results are compared also with NPs after PEGylation.

The relaxation time values of Gd-DTPA and cHANPs are first calculated at 37°C and 1.5 T (Minispec mq60). For all magnetic resonance instruments, results clearly show that the relaxation time for Gd-DTPA entrapped within cHANPs is shorter than that of the 'free' CA.

Also in these conditions, after PEGylation for both strategies, we have achieved a T_1 of 1590 ms which corresponds to 20 µM of Gd-loaded cHANPs suspension (measured through ICP-MS), while 100 µM of Gd-DTPA free in solution is required to achieve a comparable T_1 (Figure 6). Indeed, the relaxation time reported for cHANPs is achieved with a concentration about five-times lower than that of the free Gd-DTPA.

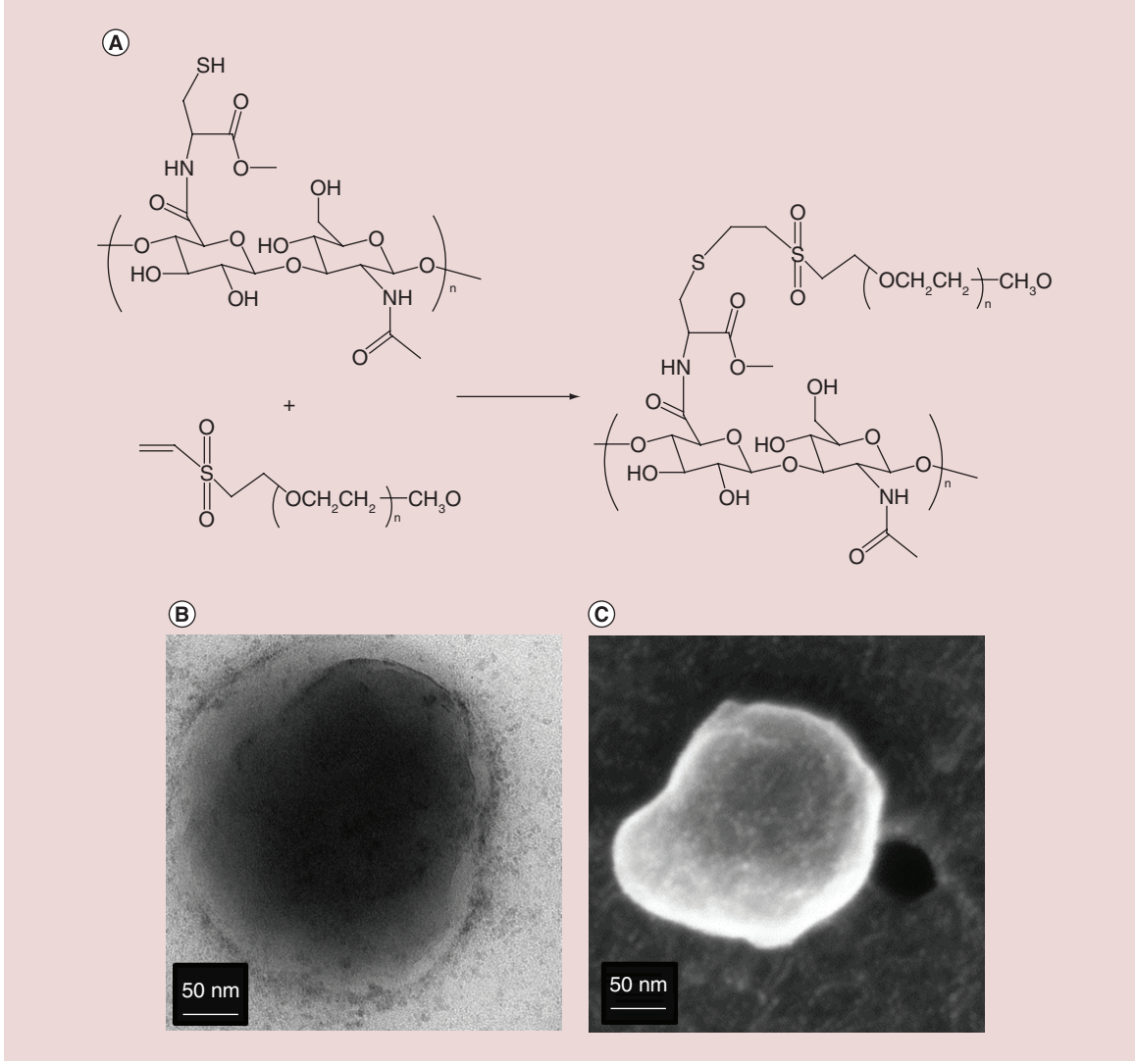

Figure 4. HA-PEG-VS reaction in microfluidics. **(A)** Schematic illustration of the Michael addition reaction mechanism of thiolated HA with PEG-VS. **(B)** TEM and **(C)** FE-SEM images of the PEGylated cHANPs in water after 48 h. cHANP: Crosslinked hyaluronic acid nanoparticle; FE-SEM: Field emission scanning electron microscope; TEM: Transmission electron microscope.

Discussion

Among different CAs for MRI, Gd chelates based ones, owing to its enhanced stability and paramagnetic properties, are used in up to 30% of clinical MRI scans and are considered clinically approved for human use. However, their effectiveness remains limited owing to nephrotoxicity effects, intracranial deposition [25], lack of tissue specificity, low relaxivity, short *in vivo* circulation time and poor specificity which restraints its application.

Research focusing on polymeric hybrid nanostructures for bioengineering, nanomedicine and theranostic applications has undergone drastic transformations in the past few decades. The interest of these nanosystems particularly relies on the new dimensions and new potentials they offered regarding their enhanced interactions with micro- or macro-environments. In fact, they can penetrate living tissues, and encapsulate, protect and deliver the drug into specific targeted sites. Furthermore, systems with monodisperse size under 100 nm are likely to improve delivery functions to the tissues, stability of the metal chelates and provide enhanced relaxometric properties of the Gd-based CAs. In fact, it is also highly interesting to have a monodisperse size of the core material, which is one of the most important parameters for a uniform biodistribution. Microfluidics has demonstrated its ability to improve size- and composition- control in the field of NP synthesis [11,15].

In a recent work [40], we have explored the impact of crosslinked and uncrosslinked biopolymer matrices

on relaxometric properties of CAs where the contribution to the enhancement of CAs is highlighted and attributed to the reduced mobility of water within the hydrogel. The idea was that the knowledge of these complex systems could be scaled to nanoscale dimensions, inspiring the development of a new class of nanostructured MRI CAs with highly tunable relaxometric properties. Moreover, the possibility to modulate the properties of the NPs through a flexible microfluidic platform to impact the relaxometric properties of the CAs without chemical modification of the chelates has been tested.

In the previous work [21], we have matched a nanoprecipitation phenomenon plus a crosslinking reaction in a microfluidic device for the production of cHANPs entrapping Gd-DTPA. By adding Gd to the mainstream, a significant interference is observed that we have controlled to obtain improved properties of the MRI CAs.

However, due to the increasing relevance of the multimodal imaging, the possibility to have a nanostructured system with improved relaxometric properties and simultaneous imaging modalities, controlled release and delivery behavior is required for a successful diagnosis and therapy.

In this perspective, after the optimization of the Gd-DTPA entrapment within the cHANPs as previously reported, we have performed a successful simultaneous encapsulation of free dyes with the aim to confirm the versatility of our designed microfluidic platform. ATTO 633 or ATTO 488, were simultaneously encapsulated together with Gd-DTPA providing the possibility to perform not only a boosted MRI imaging but also a multimodal imaging and a therapeutic approach, eventually.

Furthermore, a batch PEGylation reaction has been conducted on the cHANPs put forward our structures for an *in vivo* long circulation half-life. Indeed, owing to its high binding affinity for CD44, which is abundant in the tumor tissue, HA has been extensively investigated for the development of tumor targeted imaging agents and drug delivery systems [41]. However, it is worthy of note that the targetability of HA is compromised by its binding to other receptors in normal organs, such as the LYVE-1 receptor on cells located in the lymphatics and the HARE receptor on liver sinusoidal endothelial cells [42]. Therefore, it can be expected that modulation of the binding affinity of HA to the receptors may affect *in vivo* biodistribution and, eventually, targetability by a combination of active and passive targeting mechanisms. After the optimization of the encapsulation, aiming to control delivery properties of cHANPs by PEGylation, different PEGylation reactions are performed for the cHANPs, confirming an enhancement of the MRI signal of about five-times, even after the PEGylation reaction. Preliminary studies about *in vitro* toxicity and MRI acquisition highlight the powerful effect of

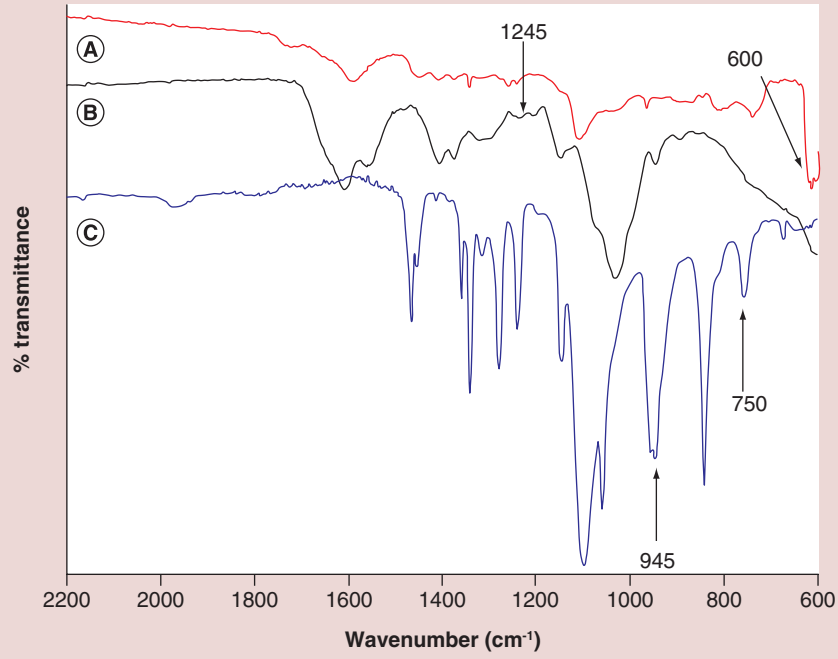

Figure 5. Fourier transform infrared spectra analysis. Comparison of FT-IR spectra of **(A)** PEGylated cHANPs, **(B)** HA-SH and **(C)** PEG-VS precursors.
cHANP: Crosslinked hyaluronic acid nanoparticle; FT-IR: Fourier transform infrared

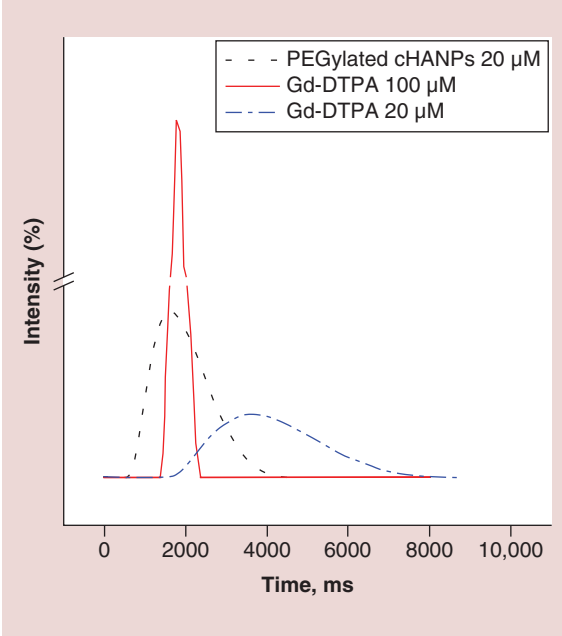

Figure 6. *In vitro* relaxation time distribution.
Relaxation time distribution reported for Gd-DTPA in water solution at 20 and 100 μM; PEGylated loaded cHANPs at standard conditions obtained using 4% v/v DVS in the side channels, at pH 12.3, reported at 20 μM of Gd-DTPA.
cHANP: Crosslinked hyaluronic acid nanoparticle; DVS: Divinyl sulfone.

the produced nanostructures for application in clinical imaging.

In addition, the platform is exploited to synthesize in a one-step manner biocompatible PEGylated cHANPs starting by HA and PEG-VS, entrapping Gd-DTPA and several types of fluorophores for application in diagnostics and therapy. The exceptional strength of the proposed work, compared with other investigations related to the formation of nanostructures, is the ability to generalize our approach to other biomaterials preserving the boosting of the relaxometric properties of the entrapped gadolinium-based CA [43]. Results show that our microfluidic approach can be applied to various other polymers maintaining unchanged process parameters in terms of optimal flow rate ratio and range concentration to obtain easily several polysaccharide NPs in a one-step manner, providing a careful control of the NP characteristics.

Conclusion

Several efforts have been recently reported about the possibility to increase the relaxivity of the CAs for MRI without the chemical modification of the chelates. Here, we investigated how hydrogel characteristics tuned through a microfluidic flow focusing approach can impact on the relaxometric properties of MRI CAs.

Our microfluidic platform confirms its effectiveness in the production of stable NPs that can entrap one or more active compounds for multimodal imaging or theranostic applications. The stability achieved in the proposed microfluidic flow focusing approach enables the post processing PEGylation of the cHANPs avoiding the release of the cargo. Furthermore, an improvement of the proposed platform is reported by presenting in a one-step strategy the synthesis of the PEGylated cHANPs entrapping Gd-DTPA and a fluorophore through a controlled co-nanoprecipitation in the microfluidic flow focusing system. PEGylated cHANPs performances have been assessed in terms of longitudinal relaxation rates: a relaxation rate T_1 of 1590 ms is achieved with 24 μM of Gd-loaded cHANPs while 100 μM of Gd-DTPA solution is required to reach similar T_1 (about 1724 ms). Results confirm the concept that the entrapment of the Gd-based CAs within the hydrogel structure can enhance relaxivity even after PEGylation reaction, thus enable potentially low administration dosage overcoming potentially several side effects related to the CAs. The proposed microfluidic platform could be applied to study the mechanisms involved in several combinations of different types of polymers and metal ions. It is important to underline that our platform is easy to move not only to the encapsulation of several drugs for a multimodal imaging or also for application in diagnostics and therapy, simultaneously. Our findings could contribute significantly to the prompt introduction of new advances in the synthesis of medical products through a high versatile microfluidic platform. In these perspectives, future outlooks are addressed to the ability to build a library of functional nanostructures on the needs of a pathology, field and material properties. Next steps are also addressed to *in vivo* study for a specific pathology and to perform an active targeting of cHANPs to reach a specific tissue.

Supplementary data

To view the supplementary data that accompany this paper please visit the journal website at: www.futuremedicine.com/doi/full/10.2217/nnm-2017-0103

Financial & competing interests disclosure

The authors have no relevant affiliations or financial involvement with any organization or entity with a financial interest in or financial conflict with the subject matter or materials discussed in the manuscript. This includes employment, consultancies, honoraria, stock ownership or options, expert testimony, grants or patents received or pending, or royalties.

No writing assistance was utilized in the production of this manuscript.

Summary points

- Highly versatile microfluidic platform to design nanostructures for application in diagnosis and therapy.
- Controlled nanoprecipitation in a microfluidic flow focusing system.
- Modulated crosslinking reaction in microfluidics.
- Simultaneous encapsulation of different active agents within nanoparticles.
- Fine-tuning of the nanoparticle' characteristics.
- Nanoprecipitation, crosslinking, encapsulation and PEGylation reaction in a one-step microfluidic process.
- Boosting of the relaxometric properties of Gd-DTPA entrapped within cHANPs and PEGylated cHANPs compared with the *free* contrast agent.

References

1 Marre S, Jensen KF. Synthesis of micro and nanostructures in microfluidic systems. *Chem. Soc. Rev.* 39(3), 1183–1202 (2010).

2 Chen KJ, Wolahan SM, Wang H *et al.* A small MRI contrast agent library of gadolinium(III)-encapsulated supramolecular nanoparticles for improved relaxivity and sensitivity. *Biomaterials* 32(8), 2160–2165 (2011).

3 Fontana F, Ferreira MPA, Correia A, Hirvonen J, Santos HA. Microfluidics as a cutting-edge technique for drug delivery applications. *J. Drug Deliv. Sci. Technol.* 34, 76–87 (2016).

4 Makgwane PR, Ray SS. Synthesis of nanomaterials by continuous-flow microfluidics: a review. *J. Nanosci. Nanotechnol.* 14(2), 1338–1363 (2014).

5 Chronopoulou L, Sparago C, Palocci C. A modular microfluidic platform for the synthesis of biopolymeric nanoparticles entrapping organic actives. *J. Nanopart. Res.* 16(11), 2703 (2014).

6 Valencia PM, Farokhzad OC, Karnik R, Langer R. Microfluidic technologies for accelerating the clinical translation of nanoparticles. *Nat. Nanotechnol.* 7(10), 623–629 (2012).

7 Valencia PM, Pridgen EM, Rhee M, Langer R, Farokhzad OC, Karnik R. Microfluidic platform for combinatorial synthesis and optimization of targeted nanoparticles for cancer therapy. *ACS Nano.* 7(12), 10671–10680 (2013).

8 Braeuer A, Dowy S, Torino E *et al.* Analysis of the supercritical antisolvent mechanisms governing particles precipitation and morphology by *in situ* laser scattering techniques. *Chem. Eng. J.* 173(1), 258–266 (2011).

9 Carvalho MR, Maia FR, Silva-Correia J, Costa BM, Reis RL, Oliveira JM. A semiautomated microfluidic platform for real-time investigation of nanoparticles' cellular uptake and cancer cells' tracking. *Nanomedicine* 12(6), 581–596 (2017).

10 Lim JM, Bertrand N, Valencia PM *et al.* Parallel microfluidic synthesis of size-tunable polymeric nanoparticles using 3D flow focusing towards *in vivo* study. *Nanomed. Nanotechnol.* 10(2), 401–409 (2014).

11 Karnik R, Gu F, Basto P *et al.* Microfluidic platform for controlled synthesis of polymeric nanoparticles. *Nano Lett.* 8(9), 2906–2912 (2008).

12 Valencia PM, Basto PA, Zhang L *et al.* Single-step assembly of homogenous lipid – polymeric and lipid – quantum dot nanoparticles enabled by microfluidic rapid mixing. *ACS Nano* 4(3), 1671–1679 (2010).

13 Kolishetti N, Dhar S, Valencia PM *et al.* Engineering of self-assembled nanoparticle platform for precisely controlled combination drug therapy. *Proc. Natl. Acad. Sci. USA* 107(42), 17939–17944 (2010).

14 Mieszawska AJ, Kim Y, Gianella A *et al.* Synthesis of polymer-lipid nanoparticles for image-guided delivery of dual modality therapy. *Bioconj. Chem.* 24(9), 1429–1434 (2013).

15 Capretto L, Cheng W, Carugo D, Katsamenis OL, Hill M, Zhang XL. Mechanism of co-nanoprecipitation of organic actives and block copolymers in a microfluidic environment. *Nanotechnology* 23(37), 16 (2012).

16 Dashtimoghadam E, Mirzadeh H, Taromi FA, Nystrom B. Microfluidic self-assembly of polymeric nanoparticles with tunable compactness for controlled drug delivery. *Polymer* 54(18), 4972–4979 (2013).

17 Majedi FS, Hasani-Sadrabadi MM, Emami SH *et al.* Microfluidic assisted self-assembly of chitosan based nanoparticles as drug delivery agents. *Lab Chip* 13(2), 204–207 (2013).

18 Anton N, Bally F, Serra CA *et al.* A new microfluidic setup for precise control of the polymer nanoprecipitation process and lipophilic drug encapsulation. *Soft Matter* 8(41), 10628–10635 (2012).

19 Ding SK, Anton N, Vandamme TF, Serra CA. Microfluidic nanoprecipitation systems for preparing pure drug or polymeric drug loaded nanoparticles: an overview. *Expert Opin. Drug Deliv.* 13(10), 1447–1460 (2016).

20 Sah E, Sah H. Recent trends in preparation of poly(lactide-co-glycolide) nanoparticles by mixing polymeric organic solution with antisolvent. *J. Nanomater.* 2015, 794601 (2015).

21 Russo M, Bevilacqua P, Netti PA, Torino E. A microfluidic platform to design crosslinked hyaluronic acid nanoparticles (cHANPs) for enhanced MRI. *Sci. Rep.* 6, 37906 (2016).

22 Kumar A. History of MRI. *J. Indian Inst. Sci.* 94(4), 363–369 (2014).

23 Xue SH, Qiao JJ, Pu F, Cameron M, Yang JJ. Design of a novel class of protein-based magnetic resonance imaging contrast agents for the molecular imaging of cancer biomarkers. *Wiley Interdiscip. Rev. Nanomed. Nanobiotechnol.* 5(2), 163–179 (2013).

24 Jonker L, Fallahi F. Patients' oral hydration levels and incidence of immediate to short-term mild side-effects in contrast agent enhanced MRI diagnostics. *Radiography* 21(2), E64–E67 (2015).

25 McDonald RJ, Mcdonald JS, Kallmes DF *et al.* Intracranial gadolinium deposition after contrast-enhanced MR imaging. *Radiology* 275(3), 772–782 (2015).

26 Gizzatov A, Stigliano C, Ananta JS *et al.* Geometrical confinement of Gd(DOTA) molecules within mesoporous silicon nanoconstructs for MR imaging of cancer. *Cancer Lett.* 352(1), 97–101 (2014).

27 Courant T, Roullin VG, Cadiou C *et al.* Hydrogels incorporating GdDOTA: towards highly efficient dual T1/T2 MRI contrast agents. *Angew. Chem. Int. Edit.* 51(36), 9119–9122 (2012).

28 Bruckman MA, Yu X, Steinmetz NF. Engineering Gd-loaded nanoparticles to enhance MRI sensitivity via T-1 shortening. *Nanotechnology* 24(46), 462001 (2013).

29 Vecchione D, Grimaldi AM, Forte E, Bevilacqua P, Netti PA, Torino E. Hybrid core-shell (HyCoS) nanoparticles produced by complex coacervation for multimodal applications. *Sci. Rep.* doi:10.1038/srep45121 (2017)(Epub ahead of print).

30 Lux F, Sancey L, Bianchi A, Cremillieux Y, Roux S, Tillement O. Gadolinium-based nanoparticles for theranostic MRI-radiosensitization. *Nanomedicine* 10(11), 1801–1815 (2015).

31 Pagel MD. The hope and hype of multimodality imaging contrast agents. *Nanomedicine* 6(6), 945–948 (2011).

32 Garcia J, Tang T, Louie AY. Nanoparticle-based multimodal PET/MRI probes. *Nanomedicine* 10(8), 1343–1359 (2015).

33 Muthu MS, Mehata AK, Viswanadh MK. Upconversion nanotheranostics: emerging designs for integration of diagnosis and therapy. *Nanomedicine (Lond.)* 12(6), 577–580 (2017).

34 Russo M, Bevilacqua P, Netti PA, Torino E. Commentary on "a microfluidic platform to design crosslinked hyaluronic acid nanoparticles (cHANPs) for enhanced MRI". *Mol. Imaging* 16, 1536012117706237 (2017).

35 Jeong CG, Francisco AT, Niu ZB, Mancino RL, Craig SL, Setton LA. Screening of hyaluronic acid-poly(ethylene glycol) composite hydrogels to support intervertebral disc cell biosynthesis using artificial neural network analysis. *Acta Biomater.* 10(8), 3421–3430 (2014).

36 Jin R, Teixeira LSM, Krouwels A *et al.* Synthesis and characterization of hyaluronic acid-poly(ethylene glycol) hydrogels via Michael addition: an injectable biomaterial for cartilage repair. *Acta Biomater.* 6(6), 1968–1977 (2010).

37 Demello J, Demello A. Microscale reactors: nanoscale products. *Lab Chip* 4(2), N N11–N15 (2004).

38 Provencher SW. CONTIN: a general purpose constrained regularization program for inverting noisy linear algebraic and integral equations. *Comput. Phys. Commun.* 27(3), 229–242 (1982).

39 Esquivel R, Juarez J, Almada M, Ibarra J, Valdez MA. Synthesis and characterization of new thiolated chitosan nanoparticles obtained by ionic gelation method. *Int. J. Polym. Sci.* 24(8), 1939–1949 (2015).

40 Ponsiglione AM, Russo M, Netti PA, Torino E. Impact of biopolymer matrices on relaxometric properties of contrast agents. *Interface Focus* 6(6), 20160061 (2016).

41 Saravanakumar G, Choi KY, Yoon HY *et al.* Hydrotropic hyaluronic acid conjugates: synthesis, characterization, and implications as a carrier of paclitaxel. *Int. J. Pharm.* 394(1–2), 154–161 (2010).

42 Choi KY, Min KH, Yoon HY *et al.* PEGylation of hyaluronic acid nanoparticles improves tumor targetability *in vivo*. *Biomaterials* 32(7), 1880–1889 (2011).

43 Utech S, Boccaccini AR. A review of hydrogel-based composites for biomedical applications: enhancement of hydrogel properties by addition of rigid inorganic fillers. *J. Mater. Sci.* 51(1), 271–310 (2016).